Thermochimica Acta 495 (2009) 120–128

Contents lists available at ScienceDirect

Thermochimica Acta

journal homepage: www.elsevier.com/locate/tca

In situ prepared PBSu/SiO_2 nanocomposites. Study of thermal degradation mechanism

A.A. Vassiliou [a], K. Chrissafis [b], D.N. Bikiaris [a,*]

[a] Laboratory of Organic Chemical Technology, Department of Chemistry, Aristotle University of Thessaloniki, GR-541 24 Thessaloniki, Macedonia, Greece
[b] Solid State Physics Section, Physics Department, Aristotle University of Thessaloniki, GR-541 24 Thessaloniki, Macedonia, Greece

ARTICLE INFO

Article history:
Received 7 April 2009
Received in revised form 4 June 2009
Accepted 10 June 2009
Available online 17 June 2009

Keywords:
Nanocomposites
Aliphatic polyester
Poly(butylene succinate)
Fumed silica
Thermal degradation
Kinetic analysis

ABSTRACT

A series of nanocomposites consisted of poly(butylene succinate) (*PBSu*) and fumed silica nanoparticles (*SiO_2*) were prepared using the in situ polymerization technique. The amount of SiO_2 used directly affected the final molecular weight of the prepared polyesters. At a low SiO_2 content (0.5 wt.%) the molecular weight obtained was higher compared to neat PBSu, however at higher concentrations this was gradually reduced. The melting point of the matrix remained unaffected by the addition of the nanoparticles, in contrast to the crystallinity, which was dramatically reduced at higher SiO_2 contents. This was mainly due to the extended branching and cross-linking reactions that took place between the carboxylic end groups of PBSu and the surface silanols of the nanoparticles. Thermal degradation of the PBSu/SiO_2 nanocomposites was studied by determining theirs mass loss during heating. From the variations of the activation energies, calculated from the thermogravimetric curves, it was clear that nanocomposites containing 1 wt.% SiO_2 content had a higher activation energy compared to pure PBSu, indicating that the addition of the nanoparticles could slightly increase the thermal stability of the matrix. However, in PBSu/SiO_2 nanocomposite containing 5 wt.% SiO_2 the activation energy was smaller. This phenomenon should be attributed to the existence of extended branched and cross-linked macromolecules, which reduce the thermal stability of PBSu, rather than to the addition of fumed silica nanoparticles.

1. Introduction

Biodegradable polymers have received a great deal of attention during the last two decades. Among the various categories of biodegradable polymers, aliphatic polyesters have attracted considerable attention due to their combination of biodegradability, biocompatibility and physical or chemical properties, which are comparable to some of the most commonly used polymers, such as LDPE, PP and HDPE. Poly(butylene succinate) (PBSu) is one of the most significant biodegradable polyesters and is, furthermore, commercially available. It can be synthesized by polycondensation of 1,4-butanediol with succinic acid. It has a relatively high-melting point, 112–114 °C, and it exhibits a controllable biodegradation rate and high processibility. Its mechanical properties, such as elongation at break and tensile strength, are comparable to those of iPP and HDPE.

The crystallization characteristics of PBSu were studied by DSC and optical microscopy and were found to closely depend on the cooling rate [1]. Its crystallization behavior is similar to that of polyethylene, with well formed lamellar morphologies. Equilibrium melting point and the glass transition temperature were found equal to about 132 and −38 °C, respectively, while the enthalpy of fusion is 200–210 J/g. By isothermal crystallization using DSC, the equilibrium melting point of PBSu was found to be 140 °C and multiple melting peaks (up to three) have also been reported [2]. The existence of two different kinds of crystals, perfect, that were formed at higher temperatures, and imperfect, that were formed at low crystallization temperatures, is characteristic of most semicrystalline polyesters. A dependence of thermal properties on molecular weight was also mentioned [3]. Melting point (T_m) and crystallization temperature (T_c) are decreased by increasing the molecular weight of PBSu. In our previous work concerning the biodegradation rate of polyesters derived from succinic acid it was found that PBSu had a lower biodegradation rate compared to poly(propylene succinate) and poly(ethylene succinate) [4].

PBSu has several interesting properties, including biodegradability, melt processibility and chemical resistance, which give rise to wide range of potential applications [5–13]. However, PBSu exhibits some shortcomings, such as insufficient stiffness, low-melt strength and viscosity, and poor mechanical and thermal properties. To overcome some of these drawbacks PBSu is copolymerized with adipic acid in the present of a multifunctional glycol and the produced copolymer becomes, thus, effective for film or bottle production. This copolymer is commercially available under the trade

* Corresponding author. Tel.: +30 2310 997812; fax: +30 2310 997667.
E-mail address: dbic@chem.auth.gr (D.N. Bikiaris).

0040-6031/$ – see front matter © 2009 Elsevier B.V. All rights reserved.
doi:10.1016/j.tca.2009.06.010

name Bionolle™, supplied by Showa Polymers, Japan. Nevertheless, some of the polymer's properties, in particular mechanical, thermal and gas barrier, can also be improved by the addition of nanoparticles in the polymer matrix [14–19].

In a recent study, utilizing a grafting method, PBSu/silica nanocomposites were prepared in order to enhance the dispersibility and interfacial adhesion between the silica nanoparticles and the PBSu matrix [20]. It was found that the thermal stability, mechanical properties and rheological properties of the PBSu nanocomposites containing silica-g-PBSu were remarkably improved, due to the surface characteristics of the silica nanoparticles grafted with the PBSu molecules, which provided good compatibility and dispersion degree. A series of PBSu/silica nanocomposites were also prepared by in situ polymerization [21]. The nanocomposite containing 3.5 wt.% silica exhibited greatly improved mechanical properties. The tensile strength at break and elongation were measured at 38.6 MPa and 515%, while those of the pure PBSu were 26.3 MPa and 96%, respectively. Although it is well known that nanoparticles can enhance thermal stability of polymer matrices, there is no published work concerning PBSu nanocomposites. Furthermore, even for neat PBSu limited work has been reported so far concerning its thermal stability and thermal degradation kinetics [22,23].

The aim of the present work was to prepare PBSu/SiO_2 nanocomposites by in situ polymerization and to study the effect of the nanoparticles' content on the properties of the final material and, mainly, on the thermal degradation mechanism. For the kinetic analysis the Ozawa–Flynn–Wall and Friedman methods were used.

2. Experimental

2.1. Materials

Succinic acid (purum 99+%), 1,4-butanediol (purity >99.7%) and tetrabutyl titanate catalyst of analytical grade were purchased from Aldrich Chemical Co. Fumed silica nanoparticles (SiO_2) used for nanocomposites preparation, were supplied by Degussa AG (Hanau, Germany) under the trade name AEROSIL® 200, having a specific surface area of 200 m^2/g, SiO_2 content >99.8% and an average primary particle size of 12 nm. All other materials and solvents used for the analytical methods were of analytical grade.

2.2. In situ prepared nanocomposites

Nanocomposites of poly(butylene succinate) (PBSu) were prepared in situ by the two-stage melt polycondensation of succinic acid and 1,4-butanediol in a glass batch reactor at a molar ratio of 1:1.3 Su:Bu. Appropriate amount of filler was first dispersed in 1,4-butanediol by ultrasonic vibration (50 W, Hielscher UP50H) and intense stirring with a magnetic stirrer (300 rpm) for 10 min prior to polymerization. The polymerization mixture, after being placed in a 250 cm^3 round bottomed flask, was de-aired and purged with dry nitrogen three times. Thereupon, the mixture was heated under a nitrogen atmosphere for 3 h at 200 °C under constant stirring (350 rpm), with water removed as the reaction by-product of esterification.

Afterwards, for the second reaction stage of polycondensation, 0.3 wt.% of TPP as heat stabilizer and 1.0×10^{-3} mol per mole of succinic acid of TBT as polycondensation catalyst were added. The reaction was continued under increased mechanical stirring (720 rpm) and high vacuum (~5.0 Pa), which was applied slowly over a period of time of about 30 min, to avoid excessive foaming and to minimize oligomer sublimation, at 220 and 240 °C for 1 h intervals, respectively. Polymerization was stopped by fast cooling to room temperature. After the polycondensation reaction was completed, the polyesters were easily removed from the flask.

For the preparation of nanocomposites containing 0.5, 1, 2.5 and 5 wt.% fumed SiO_2 nanoparticles the aforementioned procedure was used, appropriately adjusting the initial SiO_2 nanoparticles' amount dispersed in the diol.

2.3. Intrinsic viscosity measurement

Intrinsic viscosity measurements of the nanocomposites were performed using an Ubbelohde viscometer cap. Oc at 25 °C in chloroform at a solution concentration of 1 wt.%. The intrinsic viscosities [η] were calculated using the Solomon–Ciuta equation:

$$[\eta] = \frac{\sqrt{2 \times (t/t_0 - \ln(t/t_0) - 1)}}{C} \quad (1)$$

where C is the concentration of the solution, t the flow time of the solution and t_0 the flow time of the solvent. In some samples an insoluble fracture was also observed. The insoluble portion was separated by filtration and washed extensively with the solvent to remove soluble macromolecules. Afterwards it was dried to constant weight under vacuum. Corrections were made on the concentration value used for the calculation of the intrinsic viscosities, due to the filler and the insoluble fraction.

2.4. Gel permeation chromatography (GPC)

GPC analysis was performed using a Waters 150C GPC equipped with a differential refractometer as detector and three ultrastyragel (103, 104, 105 Å) columns in series. $CHCl_3$ was used as the eluent (1 ml/min) and the measurements were performed at 35 °C. Calibration was performed using polystyrene standards with a narrow molecular weight distribution.

2.5. Scanning electron microscopy (SEM)

The morphology of the prepared nanocomposites was examined using a scanning electron microscopy system (SEM) type JEOL (JMS-840) equipped with an energy-dispersive X-ray (EDX) Oxford ISIS 300 micro-analytical system. The studied surfaces were coated with carbon black in order to obtain good conductivity for the electron beam. Operating conditions were: accelerating voltage 20 kV, probe current 45 nA and counting time 60 s.

2.6. Differential scanning calorimeter (DSC)

The thermal measurements were carried out using a Setaram DSC141 unit. Temperature and energy calibrations of the instrument were performed at different heating rates, using the melting temperatures and melting enthalpies of high-purity zinc, tin and indium supplied with the instrument. The samples used, which were in powder form and weighted about 7 mg, were placed in aluminium crucibles, while an empty aluminium crucible was used as reference. A constant nitrogen flow was maintained to provide a constant thermal blanket within the DSC cell, thus eliminating thermal gradients and ensuring the validity of the applied calibration standard from sample to sample. The heating rate used was 5 °C/min.

2.7. Thermogravimetric analysis

Thermogravimetric measurements were carried out using a SETARAM SETSYS TG-DTA 16/18. Samples (6.0 ± 0.2 mg) were placed in alumina crucibles. An empty alumina crucible was used as reference. PBSu and PBSu/SiO_2 nanocomposites were heated from ambient temperature to 550 °C in a 50 ml/min flow of N_2 at heating rates of 5, 10, 15 and 20 °C/min. Continuous recordings of sample

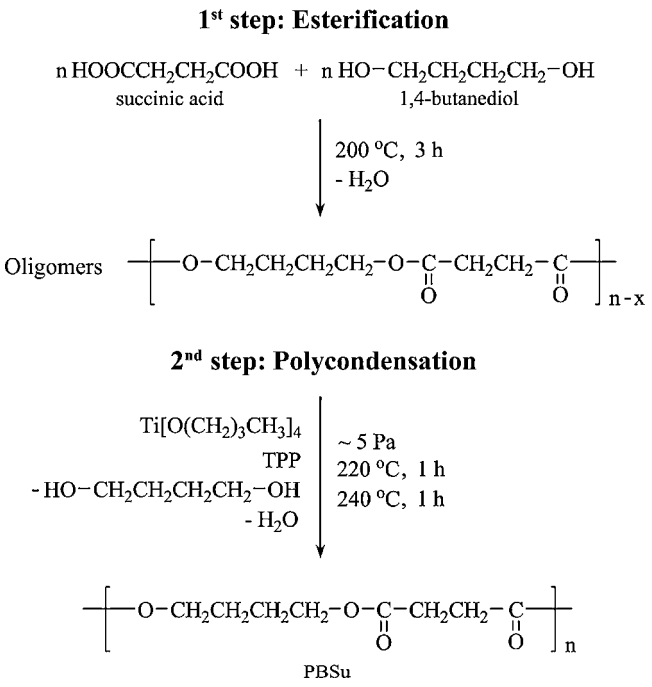

Fig. 1. Synthetic route for the preparation of poly(butylene succinate) via the two-step polycondensation technique.

temperature, sample weight, its first derivative and heat flow were taken.

3. Results and discussion

3.1. Characterization of in situ prepared PBSu/SiO_2 nanocomposites

The reactions that took place during synthesis of PBSu and its nanocomposites are presented in Fig. 1. During the first stage of esterification oligomers were prepared, which had molecular weights ranging between 1500 and 2000 g/mol, while water was removed as the reaction's by-product [4]. In order to prepare polyesters of high molecular weight, the polycondensation of these oligomers ensued at a higher temperature, with the simultaneous application of high vacuum. The number average molecular weight of PBSu that was obtained following the aforementioned procedure was 57,000 g/mol, which is quite satisfactory for aliphatic polyester. The presence of the SiO_2 nanoparticles in the polymerization mixture, as in the case of poly(ε-caprolactone) [24], affected the reaction, leading to variations of the final molecular weight of the synthesized polymers. As shown in Table 1, the average molecular weight of the nanocomposites fluctuated. Initially the molecular weight was increased for a SiO_2 concentration of 0.5 wt.%, followed by a gradual decrease at higher concentrations. However, in all nanocomposites, except for the one containing 5 wt.% SiO_2, the measured molecular weights were higher compared to pure PBSu.

As found from our previous study on the alipharomatic polyester poly(ethylene terephthalate), the silanol (≡Si–OH) surface groups of SiO_2 nanoparticles could react with the end groups of polyesters [25]. Such a reaction was also verified in PBSu and results from solid-state ^{29}Si NMR of PBS/silica, as well as from FTIR indicated a covalent bonding between Si and the PBSu polymer backbone chain [26]. Similar reactions, between the surface silanol groups of the fumed silica nanoparticles and the carboxylic end groups of PBSu, as verified by NMR spectroscopy, also took place in the present samples, prepared by the in situ technique [27]. At a low SiO_2 concentration the nanoparticles could act as chain extenders, increasing the molecular weight of the polyester, and, thus, macromolecules with higher molecular weight than pure polyester were produced [28], as in the nanocomposite containing 0.5 and 1 wt.% SiO_2. However, at higher concentrations, due to extended reactions, branched and/or cross-linked macromolecules could be formed, since SiO_2, due to the surface hydroxyl groups, can act as a multifunctional agent, leading to a partially reduction of molecular weight [25], as in nanocomposites containing 2.5 and 5 wt.% SiO_2. Branched polymers generally have lower intrinsic viscosities than the corresponding linear ones having the same molecular weight [54]. This happens because the hydrodynamic dimensions of branched macromolecules, which is what the methods used for the determination of the molecular weight actually measure, are smaller in solution than linear ones with the same molecular weight [55].

3.2. Morphological examination

Most of the nanocomposite's properties are related to the nanoparticles' dispersion degree into the polymer matrix. SiO_2 nanoparticles were added prior to the esterification reaction and it was believed that these nanoparticles would react with 1,4-butanediol, leading to a finer dispersion and, probably, the nanoparticles could be dispersed in their individual particles, having a diameter of 12 nm. However, as can be seen in Fig. 2, some aggregates were formed in all the nanocomposites. This is very common in the case when such nanoparticles are dispersed in non-polar polymers, such as polyethylene and polypropylene [29–31]. The particle sizes of these aggregates were directly related to the SiO_2 concentration. At low concentrations of 0.5 and 1 wt.% the nanoparticles showed better dispersion with agglomerates of a maximum diameter less than 100 nm. Only at concentrations of 2.5 and 5.0 wt.% some agglomerates of higher sizes were observed, though they did not exceed 200 nm in diameter. These agglomerates were formed due to the interactions between the surface silanol groups of different SiO_2 nanoparticles [32] and it seems that the interactions with the PBSu macromolecules were not sufficient to overcome this and disperse the nanoparticles as individual particles.

3.3. Thermal analysis

The DSC thermograms of PBSu/SiO_2 nanocomposites during the first heating, at a rate of 5 °C/min, are presented in Fig. 3. The melting point of pure PBSu was at 116.7 °C. From the melting enthalpy it was calculated that the polymer had a crystallinity degree of 52.0%, taking into account that the fully crystalline material has a heat

Table 1
Intrinsic viscosity, molecular weights and insoluble content of the prepared PBSu/SiO_2 nanocomposites.

Sample	$[\eta]$ (dL g^{-1})	$\bar{M}_n$ (g/mol)	$\bar{M}_w$ (g/mol)	$\bar{M}_w/\bar{M}_n$	Insoluble content (wt.%)
PBSu	1.24	57,000	126,000	2.2	–
PBSu + 0.5 wt.% SiO_2	1.90	108,500	298,500	2.8	–
PBSu + 1.0 wt.% SiO_2	1.66	89,000	230,500	2.6	–
PBSu + 2.5 wt.% SiO_2	1.40	67,500	155,500	2.3	–
PBSu + 5.0 wt.% SiO_2	1.16	54,000	116,000	2.1	3.2

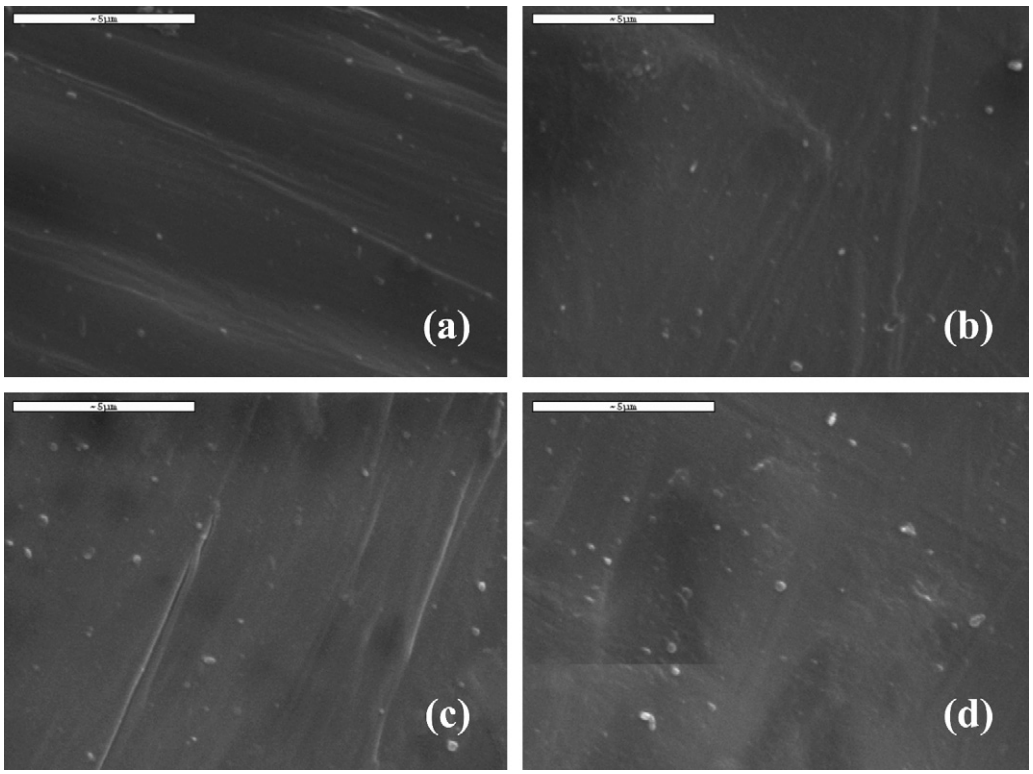

Fig. 2. SEM micrographs of PBSu/SiO_2 nanocomposites containing (a) 0.5 wt.% SiO_2, (b) 1 wt.% SiO_2, (c) 2.5 wt.% SiO_2 and (d) 5 wt.% SiO_2.

of fusion 210 J/g [33]. With the addition of the SiO_2 nanoparticles the melting point did not appear substantially affected. As seen, the melting points are very close to each other and the recorded differences are within the range of experimental error. However, the degree of crystallinity was found to be gradually reduced as the concentration of the nanoparticles increased. For nanocomposites containing 1 wt.% SiO_2 nanoparticles the calculated degree of crystallinity was 37%, while for the sample with 5 wt.% of SiO_2 the degree of crystallinity was 29.8%. Even thought it was found that SiO_2 could increase the crystallization rate of a crystalline polymer [34], it seems that in this case the nanoparticles had a negative effect on the degree of crystallinity. Such a behavior was also observed when SiO_2 nanoparticles were incorporated in HDPE, whereat the crystallization rates of the nanocomposites were faster compared to pure HDPE, but the degree of crystallinity was reduced [35]. Similar observations were reported for other PBSu nanocomposites [36,37]. Another reason that could explain why the degree of crystallinity was dramatically reduced for the sample containing 5 wt.% SiO_2 is the presence of extended branched and cross-linked structures, which impede, to a certain extent, the movement of macromolecular chains between them and reduce their freedom to move so that they can acquire the appropriate orientation as required by the crystallization process.

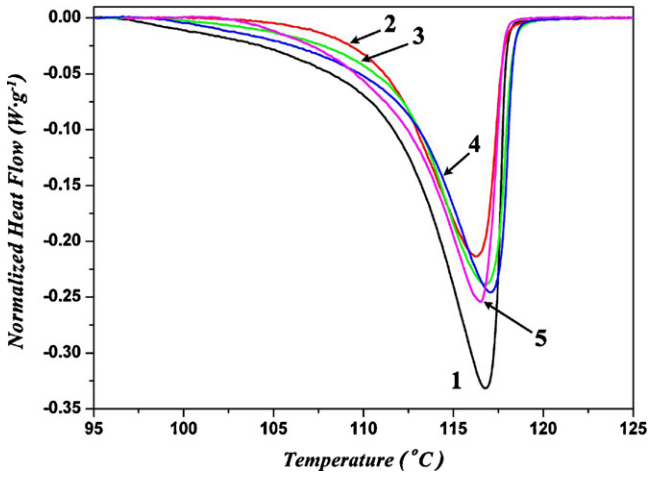

Fig. 3. Heat flow versus temperature of PBSu/SiO_2 nanocomposites. (1) PBSu, (2) PBSu + 0.5 wt.% SiO_2, (3) PBSu + 1 wt.% SiO_2, (4) PBSu + 2.5 wt.% SiO_2 and (5) PBSu + 5 wt.% SiO_2.

3.4. Kinetics of thermal degradation of PBSu/SiO_2 nanocomposites

Thermal degradation of PBSu and its nanocomposites with SiO_2 was studied by determining their mass loss during heating. In Fig. 4 the mass loss (%) and the derivative mass loss (DTG) curves of all studied samples are presented at a heating rate of 10 °C/min. From the thermogravimetric curves it can be seen that PBSu and PBSu/SiO_2 nanocomposites presented a relative good thermostability, since the maximum mass loss occurring up to a temperature of 275 °C was smaller than 0.5 wt.%. Only for the sample PBSu with 5 wt.% SiO_2 a slight increase of the observed mass loss at this temperature could be identified; 0.7 wt.% instead of 0.5 wt.% observed for the other samples. As can be seen from the peak of the first derivative, the temperature at which the decomposition rate of PBSu was at its highest was at T_p = 399.2 °C. This temperature was slightly shifted to higher values in nanocomposites containing up to 2.5 wt.% SiO_2, while the one containing 1 wt.% SiO_2 exhibited the maximum shift (4 °C). This is an indication that the SiO_2 nanoparticles stabilized the decomposition of PBSu. However, this trend was not continuous and, thus, for the sample containing 5 wt.% SiO_2 a slight decrease (T_p = 392.8 °C) was observed. This decrease should be attributed to the branched and cross-linked macromolecules that this particular sample contained, which exhibit lower thermal stability than the respective linear.

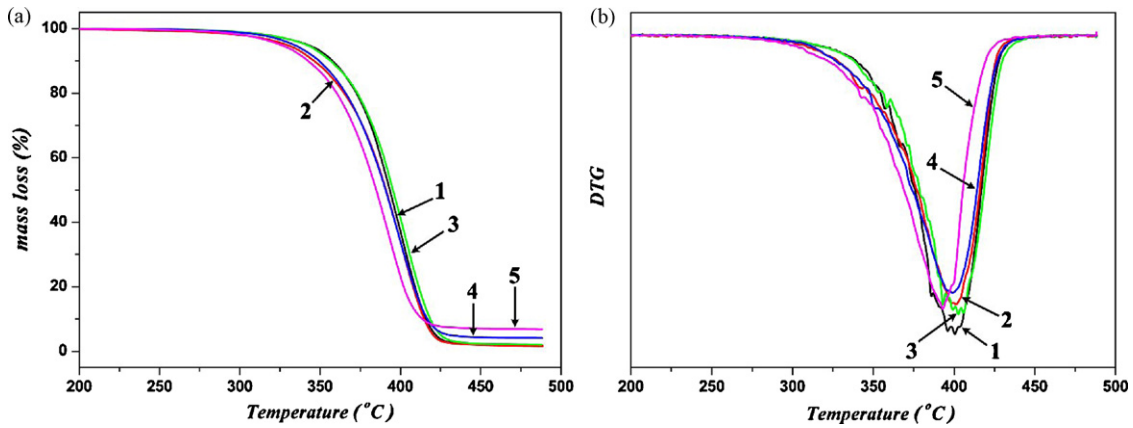

Fig. 4. (a) Mass loss (%) versus temperature and (b) derivative mass loss (DTG) versus temperature at a heating rate of $\beta = 10\,^{\circ}C/min$, for all the studied samples. (1) PBSu, (2) PBSu + 0.5 wt.% SiO_2, (3) PBSu + 1 wt.% SiO_2, (4) PBSu + 2.5 wt.% SiO_2 and (5) PBSu + 5 wt.% SiO_2.

The quantity of the final residue was larger in nanocomposites from the residue of pure PBSu, being directly depended on the SiO_2 content. The remaining residue at 475 °C in these samples was 1.7% for PBSu and 2.5%, 4.1% and 6.8% for PBSu/SiO_2 nanocomposites containing 1, 2.5 and 5 wt.% SiO_2, respectively. The additional residue is close to the incorporated SiO_2 amount.

3.4.1. Determination of the activation energy using isoconversional methods

In order to analyze more thoroughly the effect of the different concentrations of SiO_2 on the degradation mechanism of PBSu it was important that the kinetic parameters (activation energy E and pre-exponential factor A) and the conversion function $f(\alpha)$ were evaluated. The relationship between kinetic parameters and degree of conversion (α)—partial mass loss—can be found using the mass loss curves recorded in the TG measurements. Apart from pure PBSu the nanocomposites containing 1 and 5 wt.% SiO_2 were studied, since the observed differences between this contents and the other two (0.5 and 2.5 wt.% SiO_2) seems to be negligible. The degradation of these samples was studied through non-isothermal measurements at different heating rates (5, 10, 15, 20 °C/min). In Fig. 5 the mass loss (%) and the derivative mass loss at different heating rates for the PBSu/SiO_2 nanocomposite containing 1 wt.% SiO_2 are presented as a representative example.

For the determination of the activation energy, isoconversional methods were used [38–41]. These are in fact "model free" methods which assume that the conversion function $f(\alpha)$ does not change with the variation of the heating rate for all values of the degree of conversion α (partial mass loss). They involve the measuring of the temperatures corresponding to fixed values of α by experiments at different heating rates β. The isoconversional methods are considered to give accurate values of the activation energy. The pre-exponential factor usually cannot be determined without the assumption of the reaction model ($f(\alpha)$). Two of these methods were used for reasons of comparison. The first one was the Ozawa–Flynn–Wall (OFW) method [42–44] and the second one the Friedman method [45,46].

The results of the two methods are shown in Fig. 6 for the studied PBSu/SiO_2 nanocomposites. From the plots it can be seen that although the shape of the curves was almost the same, significant differences could be recognized at the activation energy values for the same value of partial mass loss. The differences in the values of E calculated by the OFW and Friedman methods, for the same sample, can be explained by a systematic error due to improper integration. The method of Friedman employs instantaneous rate values being, therefore, very sensitive to experimental noise. With the OFW method, the equation used is derived assuming constant activation energy and by introducing systematic error in the estimation of E in the case that E varies with α, an error that can be estimated by comparison with the Friedman results [47].

From these calculations the variations of the activation energy can be measured. It is clear from the plots that the mean value of the activation energy of PBSu is different from its nanocomposites. Thus, the sample containing 1 wt.% SiO_2 content had higher activation energy, which is evidence that the addition of the nanoparticles could slightly increase the thermal stability of the PBSu matrix.

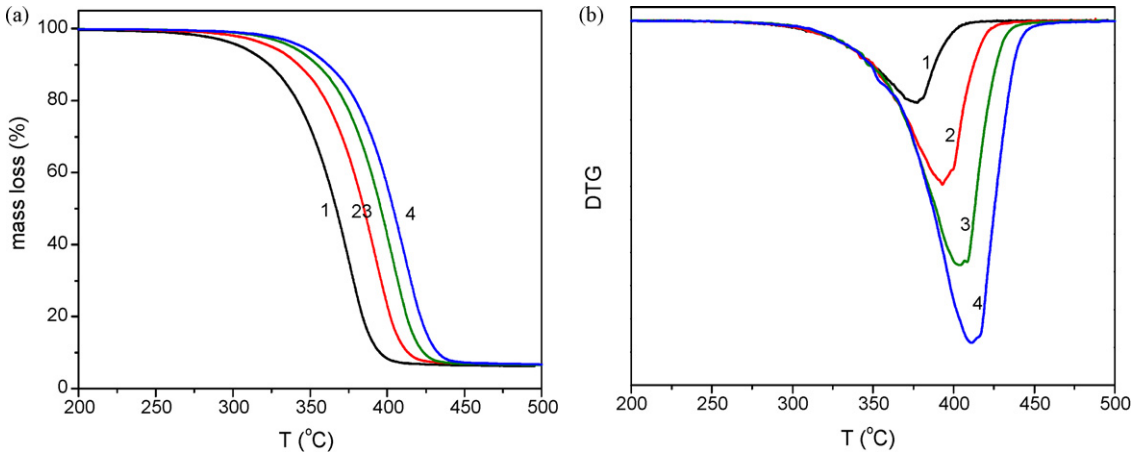

Fig. 5. (a) Mass loss (%) and (b) derivative mass loss (DTG) curves of PBSu nanocomposite with 1 wt.% SiO_2 at different heating rates. (1) $\beta = 5\,^{\circ}C/min$, (2) $\beta = 10\,^{\circ}C/min$, (3) $\beta = 15\,^{\circ}C/min$ and (4) $\beta = 20\,^{\circ}C/min$.

This is usual in polymer matrices containing nanoparticles, since the produced gases during decomposition are more difficultly liberated from matrices containing inorganic particles like SiO_2 [48,49]. However, in the case of the PBSu/SiO_2 nanocomposite containing 5 wt.% SiO_2 content the activation energies were smaller. This phenomenon can be attributed to the existence of extended branched and cross-linked macromolecules at this particular sample, rather than to the silica addition.

It can be educed from Fig. 6 that the dependence of E on α could be separated in two distinct regions. For the PBSu sample the first region extended up to $\alpha = 0.1$, whereat a rapid increase of the activation energy was observed, and the second one for $\alpha > 0.1$, whereat the activation energy could be considered as having the same value. In the first region for the PBSu/SiO_2 nanocomposite containing 5 wt.% SiO_2 an increase of the activation energy was also exhibited up to $\alpha = 0.3$, at a lower rate compared to pure PBSu, and in the second region E presented a more or less slight increase. The same trend was also observed for the nanocomposite containing 1 wt.% SiO_2, which at the first stages exhibited a slightly lower activation energy compared to pure PBSu, but at higher conversions the activation energy was higher compared to the corresponding of pure PBSu. If the determined activation energy is the same for the various values of α, the existence of a single-step reaction could be concluded with certainty. On the contrary, a change of E with increasing degree of conversion is an indication of a complex reaction mechanism that invalidates the separation of variables involved in the OFW analysis [50]. These complications are significant, especially in the case when the total reaction involves competitive mechanisms. From the above it is clear that according to Fig. 5 there was an indication of a complex reaction with the participation of at least two different mechanisms, from which one had quite a small effect on mass loss. The "two mechanisms"—as a result of the increasing E with a—is a rather typical phenomenon of many polymers [51,52]. From the two mechanisms the first corresponded to the part where small mass loss appeared, while the second part, where the substantial mass loss took place, was attributed to the main decomposition mechanism, each mechanism presenting different activation energy.

3.4.2. *Determination of the conversion function $f(\alpha)$ using model fitting*

For the determination of the conversion function $f(\alpha)$, since it could not be determined with the isoconversional methods, a model fitting method was used [49,53–55]. This method involves

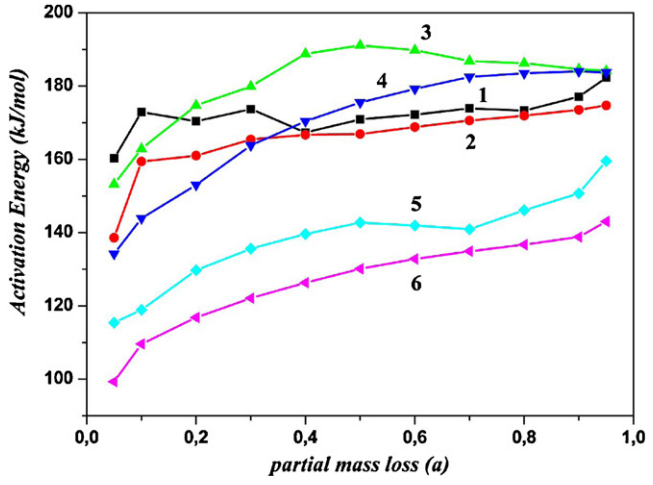

Fig. 6. Dependence of the activation energy (E) on the degree of the partial mass loss (α), as calculated with Friedman and OFW methods for PBSu (1 and 2), PBSu/SiO_2 1 wt.% (3 and 4) and PBSu/SiO_2 5 wt.% (5 and 6) nanocomposites.

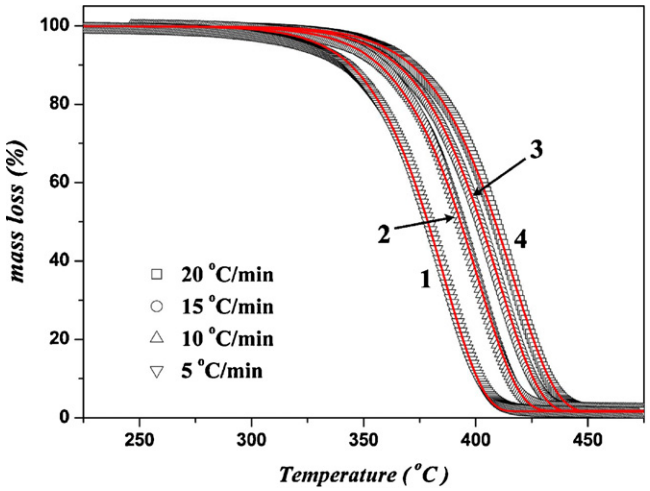

Fig. 7. Mass loss (%) of pure PBSu and fitting curves with the Fn reaction model for different heating rates. (1) $\beta = 5\,^{\circ}$C/min, (2) $\beta = 10\,^{\circ}$C/min, (3) $\beta = 15\,^{\circ}$C/min and (4) $20\,^{\circ}$C/min.

fitting different models to α-temperature curves and simultaneously determining the activation energy E and the pre-exponential factor A. The method that was used is the "multivariate non-linear regression method" [56,57]. In order to determine the nature of the mechanisms through the comparison of the experimental and theoretical data, initially it was considered that the degradation of the polyester could be described only by a single mechanism that corresponded to the main mass loss, without presuming the exact mechanism. If the result of the fitting could not be considered as acceptable, then we would have proceeded to fit the experimental data with a combination of two mechanisms. It has been shown that model fitting to multiple heating rates data gives activation energies similar to the values estimated by the isoconversional methods [41].

In a previous article we had presented the kinetics of PBSu [22]. For this reason, in this article we were mainly focused on the study of the kinetics of PBSu nanocomposites containing 1 and 5 wt.% SiO_2. Furthermore, we present more details about the kinetics of the PBSu and we compare these results with the analogous ones for PBSu/SiO_2 nanocomposites. Examining the literature it can be concluded that for the kinetic description of the thermal degradation of the polymers two kinetic models have mainly been used, the first-order (F1) and the nth-order (Fn). For the calculation of the activation energy, single or multiple heating rate data have also been used. Firstly, for the fitting of the mass loss experimental curve, F1 and Fn reaction models were used. In Fig. 7 the results of the fitting using the Fn model can be seen for pure PBSu, since the fit using F1 model was not acceptable. From this figure it was obvious that when more than one set of data from different heating rates were used, the reaction models Fn gave an almost acceptable fit. Only small divergences could be observed at a small first area of mass loss and, especially, for a lower heating rate. The same procedure of fitting was also carried out for the PBSu nanocomposite containing 1 and 5 wt.% SiO_2. For reasons of comparison the fitting with the Fn model for the nanocomposite containing 5 wt.% SiO_2 is presented in Fig. 8.

From Fig. 8 it is obvious that the divergences were not only in the small first area of mass loss as for the PBSu sample. The first area is now up to $\alpha = 0.3$ and, also, another area with divergences were observed at the end of the degradation for all the heating rates. This observation was in accordance with the steps of the dependence of the activation energy from α (Fig. 6). Although the fitting of pure PBSu could be considered as an accepted one the same thing was not possible for the PBSu nanocomposite con-

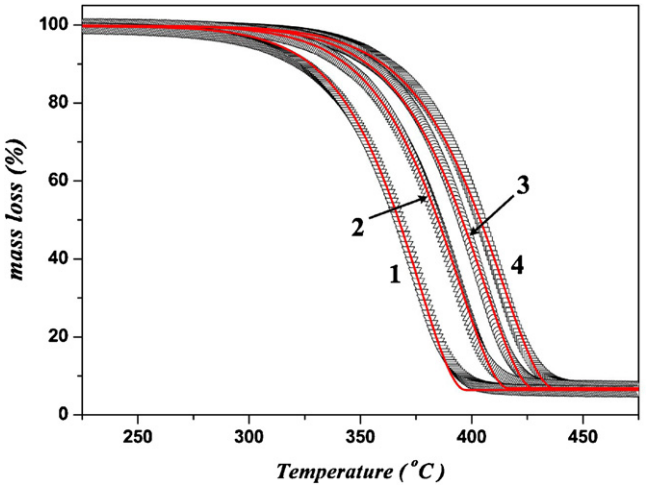

Fig. 8. Mass lose (%) of PBSu nanocomposite containing 5 wt.% SiO_2 and fitting curves with the Fn reaction model for different heating rates. (1) $\beta = 5\,^{\circ}C/min$, (2) $\beta = 10\,^{\circ}C/min$, (3) $\beta = 15\,^{\circ}C/min$ and (4) $\beta = 20\,^{\circ}C/min$.

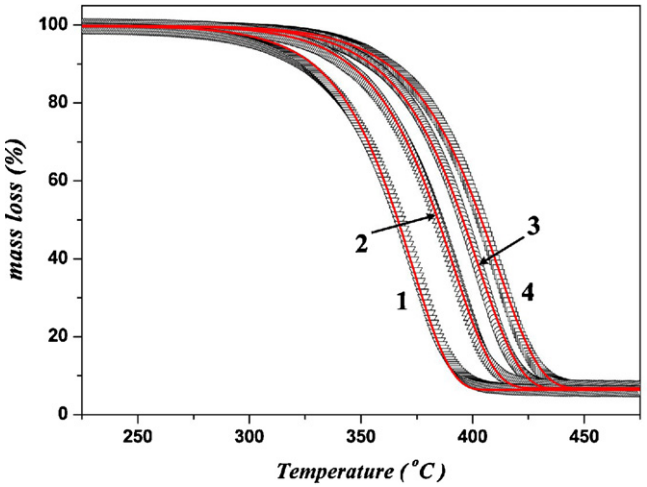

Fig. 9. Mass loss (%) of PBSu nanocomposite containing 5 wt.% SiO_2 and fitting curves with the Cn reaction model for different heating rates. (1) $\beta = 5\,^{\circ}C/min$, (2) $\beta = 10\,^{\circ}C/min$, (3) $\beta = 15\,^{\circ}C/min$ and (4) $\beta = 20\,^{\circ}C/min$.

taining 5 wt.% SiO_2. In order to improve the quality of the fitting, mainly for the PBSu nanocomposite containing 5 wt.% SiO_2, 16 different reaction models were examined. The form of the conversion functions, obtained by the best fitting for the PBSu and PBSu/SiO_2 nanocomposites, were: (1) nth-order reaction with autocatalysis (Cn) for which $f(\alpha) = (1-\alpha)^n(1 + K_{cat}X)$, where K_{cat} is a constant and X the reactants, (2) expanded Prout–Tompkins equation (Bna) with $f(\alpha) = (1-\alpha)^n\alpha^m$ and (3) nth order reaction (Fn) with $f(\alpha) = (1-\alpha)^n$.

These best fitting reaction models gave the same regression parameter for the PBSu/SiO_2 nanocomposites and the calculated values for the activation energy, the pre-exponential factor and the reaction order are presented in Table 2. Since the regression factor is the same, thus, the calculated values are also the same. For the PBSu/SiO_2 1 wt.% sample the best fitting was by the Fn model but the differences among the fittings by the three models were small. For the PBSu/SiO_2 5 wt.% sample the best fitting was by the Cn model but, as in the case of PBSu/SiO_2 1 wt.%, the differences between the fittings by the three models were small. These small differences also give small differences for the calculated values. For comparison reasons the fitting with the Cn model is presented in Fig. 9.

Comparing the results of the fitting with the Fn and Cn models for the PBSu nanocomposites it is obvious that the Cn model fitted the experimental data better, especially at the end of the mass loss, although better fitting results were also obtained for the first region of mass loss and for heating rates greater than 5 °C/min. Comparing the results of the fitting for the pure PBSu and its nanocomposites with the Cn model it is obvious that the quality of the fitting for the pure PBSu is better than that for its nanocomposites.

Although the fitting of PBSu could be considered as an acceptable one, the same could not stand for the PBSu/SiO_2 nanocomposites. In order to improve the quality of the fitting, mainly for the PBSu nanocomposites, using the conclusions from the dependence of the activation energy from the partial mass loss, two reaction mechanisms should be used, in order to improve the quality of the fitting. For comparison reasons, two reaction mechanisms were also used for pure PBSu.

For the determination of the mechanism at the first mass loss area for pure PBSu and its nanocomposites, the following were assumed: (a) the two mechanisms are consecutive and (b) this mechanism, which we try to identify, corresponds to a small mass loss, according to the experimental results. In the process of identification by two different mechanisms, at least six unknown factors

Table 2
Activation energy, pre-exponential factor and reaction order for Fn, Bna and Cn reaction models for PBSu and its nanocomposites containing 1 and 5 wt.% SiO_2.

Reaction model	Activation energy (kJ/mol)	Pre-exponential factor (s^{-1})	Reaction order (n)	
PBSu				
Fn	165.3	10.67	0.78	
Bna	165.4	10.68	0.78	7.3E−6[a]
Cn	164.3	10.58	0.86	−0.68[b]
PBSu/SiO_2 1 wt.% SiO_2				
Fn	169.7	11.0	0.82	
Bna	169.6	11.0	0.82	7.1E−6[a]
Cn	169.7	11.0	0.82	−3.6[b]
PBSu/SiO_2 5 wt.% SiO_2				
Fn	131.7	8.08	0.53	
Bna	130.0	7.99	0.60	5.3E−2[a]
Cn	128.8	7.79	0.82	−1.8E−2[b]

Fn, nth-order reaction; Bna, Prout–Tompkins equation; Cn, nth-order reaction with autocatalysis.
[a] Exponent m.
[b] $\log K_{cat}$.

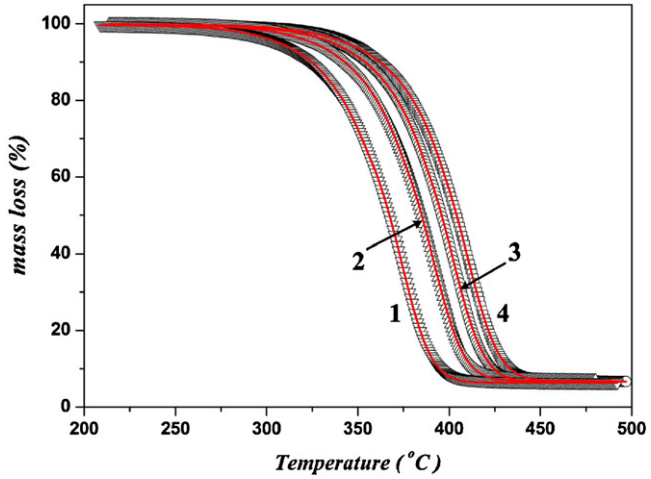

Fig. 10. Mass loss (%) of pure PBSu and fitting curves for different heating rates and for two consecutive reactions mechanism. (1) $\beta = 5\,^{\circ}C/min$, (2) $\beta = 10\,^{\circ}C/min$, (3) $\beta = 15\,^{\circ}C/min$ and (4) $\beta = 20\,^{\circ}C/min$.

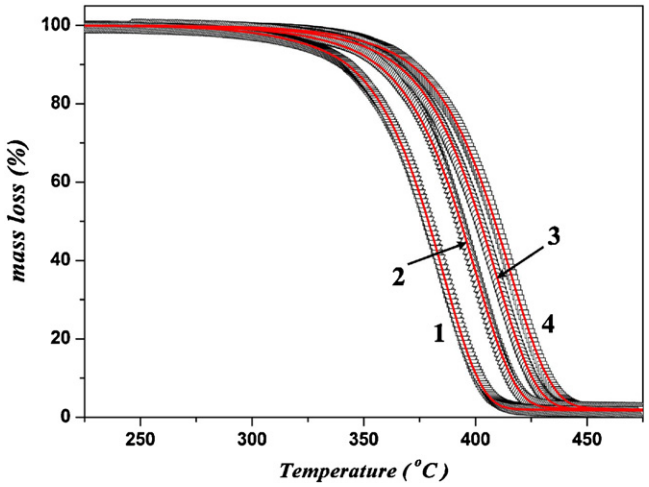

Fig. 11. Mass loss (%) of PBSu nanocomposite containing 5 wt.% SiO_2 and fitting curves for different heating rates and for two consecutive reactions mechanism. (1) $\beta = 5\,^{\circ}C/min$, (2) $\beta = 10\,^{\circ}C/min$, (3) $\beta = 15\,^{\circ}C/min$ and (4) $\beta = 20\,^{\circ}C/min$.

are involved with the mathematical problem of identification being very complex, with several possible solutions. For this reason, at this stage of identification, it is important to somewhat limit the extent of the search among all possible combinations of the 16 widely used models. So the models that were used and their combinations were only those which had given us satisfactory results from the identification through a single mechanism, such as the reaction models Fn, Cn and Bna. The fitting with two consecutive mechanisms led to a remarkable improvement in the fitting of the experimental results with the theoretical ones. Two characteristic examples are presented in Figs. 10 and 11 for pure PBSu and its nanocomposite containing 5 wt.% SiO_2. In this stage of identification, for the best possible results we left the parameters (E, A and n) of the second mechanism to be recalculated. The theoretical data fitted very well the experimental data in the first area of small mass loss.

Table 3
Activation energy, pre-exponential factor and reaction order for pure PBSu and PBSu/SiO_2 nanocomposites after fitting with two consecutive reaction mechanisms.

Model	Mechanism	Activation energy (kJ/mol)	Pre-exponential factor (s^{-1})	Reaction order (n)	
PBSu					
Fn	First	128.0	8.8	1.64	
Bna	Second	173.6	11.4	0.84	0.05[a]
Fn	First	129.8	9.0	1.65	
Cn	Second	174.1	11.4	0.84	−1.18[b]
Cn	First	126.0	8.8	1.68	−0.20[b]
Cn	Second	173.0	11.3	0.86	−0.78[b]
Fn	First	127.5	8.7	1.63	
Fn	Second	175.0	11.5	0.82	
PBSu/SiO_2 1 wt.% SiO_2					
Fn	First	123.0	7.9	0.74	
Bna	Second	183.0	12.2	1.01	0.22[a]
Fn	First	128.6	8.4	0.64	
Cn	Second	183.0	12.0	1.05	−0.12[b]
Cn	First	128.4	8.4	0.65	−1.4[b]
Cn	Second	183.0	12.0	1.05	−0.12[b]
Fn	First	121.6	7.9	0.86	
Fn	Second	185.0	12.2	0.88	
PBSu/SiO_2 5 wt.% SiO_2					
Fn	First	109.7	6.8	0.39	
Cn	Second	140.8	8.6	1.13	0.52[b]
Cn	First	109.7	6.8	0.39	−36.9[b]
Cn	Second	140.8	8.6	1.13	0.52[b]
Fn	First	96.5	5.6	0.67	
Bna	Second	140.0	9.3	1.17	0.94[a]
Fn	First	122.7	7.5	0.5	
Fn	Second	145.0	9.3	0.86	

[a] Exponent m.
[b] $\log K_{cat}$.

The identification using four different combinations of mechanisms provided for neat PBSu almost the same quality of results with the same regression coefficient, 0.999961. For the PBSu nanocomposite containing 5 wt.% SiO_2 combinations (i) Cn–Cn, (ii) Fn–Cn and (iii) Fn–Bna gave essentially the same identification with regression coefficient 0.999979 and only the combination of Fn–Fn led to improvement of one mechanism, but worse than the other three, with a regression coefficient of 0.999913. The results of the values of activation energy, the pre-exponential factor and other variables are presented in Table 3.

Table 3 shows that for the first mechanism from the combination Cn–Cn in the case of PBSu/SiO_2 nanocomposites the $\log K_{cat}$ term was negative and very large. Thus, the Kcat factor was practically negligible and almost zero. This means that the model Cn was practically the same with the model Fn and therefore the combinations Cn–Cn and Fn–Cn were identical and gave the same values of E and A. Considering that the combination of mechanisms which gave better identification did not differ between pure PBSu and the PBSu nanocomposites, it could be assumed that three of the four studied combinations could be used, since the calculated values of E and A from any combination have no practical difference. It is worth noting however that the activation energies calculated for the first and second mechanism of the PBSu/SiO_2 5 wt.% nanocomposite are obviously lower than the corresponding of pure PBSu. This finding was similar to what was observed for the values of activation energy calculated using the methods of Friedman and OFW (Fig. 6).

4. Conclusions

The studied PBSu/SiO_2 nanocomposites prepared by the in situ polymerization had different molecular weights due to the interactions that took place between the carboxylic end groups of PBSu and the surface silanol groups of SiO_2. At low SiO_2 contents these nanoparticles acted as chain extenders, increasing the molecular weight of PBSu, while at concentrations higher than 1 wt.% the led to the formation of branched and cross-linked macromolecules, decreasing the apparent molecular weight.

The dispersion of the SiO_2 nanoparticles in the PBSu matrix was fine and some small agglomerates were formed. SiO_2 nanoparticles could act as nucleating agents affecting the crystallization rate of PBSu. However, the degree of crystallinity was reduced by the presence of the nanoparticles, due to the branched and cross-linked macromolecules that these samples contained.

Thermal stability of the PBSu/SiO_2 nanocomposites containing up to 1 wt.% nanoparticles was higher compared to pure PBSu. However, for a concentration of 5 wt.% SiO_2 nanoparticles thermal stability was lowered. This was verified from the thermogravimetric curves as well as from the calculated activation energies. The decomposition of PBSu could be described using two consecutive reactions mechanism. The first one took place at low mass loss while the second one at higher conversions. The same two consecutive reactions mechanism could also be used to describe the thermal decomposition of the prepared nanocomposites.

Acknowledgements

This research project is co-financed by E.U.-European Social Fund (75%) and the Greek Ministry of Development-GSRT (25%).

References

[1] T. Miyata, T. Masuko, Polymer 39 (1998) 1399.
[2] E.S. Yoo, S.S. Im, J. Appl. Polym. Sci. Part B: Polym. Phys. 37 (1999) 1357.

[3] M. Yasuniwa, T. Satou, J. Appl. Polym. Sci. Part B: Polym. Phys. 40 (2002) 2411.
[4] D. Bikiaris, G. Papageorgiou, D. Achilias, Polym. Degrad. Stab. 91 (2006) 31.
[5] J.J. Ihn, E.S. Yoo, S.S. Im, Macromolecules 28 (1995) 2460.
[6] Y. Ichikawa, J. Suzuki, J. Washiyama, Y. Moteki, K. Noguchi, K. Okuyama, Polymer 35 (1994) 3338.
[7] Z. Gan, H. Abe, H. Kurokawa, Y. Doi, Biomacromolecules 2 (2001) 605.
[8] Z. Qiu, T. Ikehara, T. Nishi, Polymer 44 (2003) 2799.
[9] M. Okada, Prog. Polym. Sci. 27 (2002) 87.
[10] K. Bhari, H. Mitomo, T. Enjoji, F. Yoshii, K. Makuuchi, Polym. Degrad. Stab. 62 (1998) 551.
[11] Y. Doi, K. Kasuya, H. Abe, N. Koyama, S. Ishiwatari, K. Takagi, Y. Yoshida, Polym. Degrad. Stab. 51 (1996) 281.
[12] E.S. Yoo, S.S. Im, Macromolecules 28 (1995) 2460.
[13] T. Uesaka, K. Nakane, S. Maeda, T. Ogihara, N. Ogata, Polymer 41 (2000) 8449.
[14] Y.F. Shih, T.M. Wu, J. Polym. Res. 16 (2009) 109.
[15] T. Gcwabaza, S.S. Ray, W.W. Focke, A. Maity, Eur. Polym. J. 45 (2009) 353.
[16] Y.F. Shih, L.S. Chen, R.J. Jeng, Polymer 49 (2008) 4602.
[17] M.E. Makhatha, S.S. Ray, J. Hato, A.S. Luyt, J. Nanosci. Nanotechnol. 8 (2008) 1679.
[18] Y.F. Shih, T.Y. Wang, R.J. Jeng, J.Y. Wu, C.C. Teng, J. Polym. Environ. 15 (2007) 151–158.
[19] Perrine Bordesa, Eric Polleta, Luc Avérous, Prog. Polym. Sci. 34 (2009) 125.
[20] J.S. Lim, S.M. Hong, D.K. Kim, S.S. Im, J. Appl. Polym. Sci. 107 (2008) 3598.
[21] S.I. Han, J.S. Lim, D.K. Kim, M.N. Kim, S.S. Im, Polym. Degrad. Stab. 93 (2008) 889.
[22] K. Chrissafis, K.M. Paraskevopoulos, D.N. Bikiaris, Thermochim. Acta 435 (2005) 142.
[23] J. Yang, S. Zhang, X. Liu, A. Cao, Polym. Degrad. Stab. 81 (2003) 1.
[24] A.A. Vassiliou, G.Z. Papageorgiou, D.S. Achilias, D.N. Bikiaris, Macromol. Chem. Phys. 208 (2007) 364.
[25] D. Bikiaris, V. Karavelidis, G. Karayannidis, Macromol. Rapid Commun. 27 (2006) 1199.
[26] S.I. Han, J.S. Lim, D.K. Kim, M.N. Kim, S.S. Im, Polym. Degrad. Stab. 93 (2008) 895.
[27] A.A. Vassiliou, M. Kontopoulou, D.N. Bikiaris, Polymer, submitted for publication.
[28] D.S. Achilias, D.N. Bikiaris, V. Karavelidis, G.P. Karayannidis, Eur. Polym. J. 44 (2008) 3096.
[29] D.N. Bikiaris, G.Z. Papageorgiou, E. Pavlidou, N. Vouroutzis, P. Palatzoglou, G.P. Karayannidis, J. Appl. Polym. Sci. 100 (2006) 2684.
[30] D. Bikiaris, A. Vassiliou, E. Pavlidou, P. Karayannidis, Eur. Polym. J. 41 (2005) 1965.
[31] K. Chrissafis, K.M. Paraskevopoulos, E. Pavlidou, D. Bikiaris, Thermochim. Acta 485 (2009) 65.
[32] D.N. Bikiaris, A.A. Vassiliou, Nanocomposite coatings and nanocomposite materials, in: A. Öchsner, W. Ahmed, N. Ali (Eds.), Fumed Silica Reinforced Plastics, Trans Tech Publications Ltd, Switzerland, 2009 (Chapter 4).
[33] G.Z. Papageorgiou, D.N. Bikiaris, Polymer 46 (2005) 12081.
[34] G.Z. Papageorgiou, D.S. Achilias, D.N. Bikiaris, G.P. Karayannidis, Thermochim. Acta 427 (2005) 117.
[35] T.G. Gopakumar, J.A. Lee, M. Kontopoulou, J.S. Parent, Polymer 43 (2002) 5483.
[36] Y.F. Shih, T.Y. Wang, R.J. Jeng, J.Y. Wu, D.S. Wuu, J. Appl. Polym. Sci. 110 (2008) 1068.
[37] G.X. Chen, J.S. Yoon, J. Polym. Sci. Part B: Polym. Phys. 43 (2005) 817.
[38] M.J. Starink, J. Mater. Sci. 32 (1997) 6505.
[39] M. Maciejewski, Thermochim. Acta 355 (2000) 145.
[40] S. Vyazovkin, Thermochim. Acta 355 (2000) 155.
[41] A. Burnham, Thermochim. Acta 355 (2000) 165.
[42] T. Ozawa, Bull. Chem. Soc. 38 (1965) 1881.
[43] J.H. Flynn, L.A. Wall, J. Res. Natl. Bur. Stand.: Phys. Chem. 70A (1966) 487.
[44] J.H. Flynn, L.A. Wall, Polym. Lett. 4 (1966) 232.
[45] H.L. Friedman, J. Polym. Sci. C6 (1964) 183.
[46] H.L. Friedman, J. Polym. Lett. 4 (1966) 323.
[47] Vyazovkin, J. Comput. Chem. 22 (2001) 178.
[48] K. Chrissafis, K.M. Paraskevopoulos, G.Z. Papageorgiou, D.N. Bikiaris, J. Appl. Polym. Sci. 110 (2008) 1739.
[49] K. Chrissafis, K.M. Paraskevopoulos, S.Y. Stavrev, A. Docoslis, A. Vassiliou, D.N. Bikiaris, Thermochim. Acta 465 (2007) 6.
[50] T. Ozawa, J. Thermal Anal. 2 (1970) 301.
[51] J.D. Peterson, S. Vyazovkin, C.A. Wight, Macromol. Chem. Phys. 202 (2001) 775.
[52] S. Vyazovkin, Anal. Chem. 80 (2008) 4301.
[53] K. Chrissafis, G. Antoniadis, K.M. Paraskevopoulos, A. Vassiliou, D.N. Bikiaris, Comp. Sci. Technol. 67 (2007) 2165.
[54] K. Chrissafis, K.M. Paraskevopoulos, D.N. Bikiaris, Thermochim. Acta 440 (2006) 166.
[55] D.N. Bikiaris, K. Chrissafis, K.M. Paraskevopoulos, K.S. Triantafyllidis, E.V. Antonakou, Polym. Degrad. Stab. 92 (2007) 525.
[56] E. Kaisersberger, J. Opfermann, Thermochim. Acta 187 (1991) 151.
[57] E. Kaisersberger, J. Opfermann, Laborpraxis 4 (1992) 360.